BILINGUAL PUBLISHING GROUP

Journal of Environmental & Earth Sciences
https://journals.bilpubgroup.com/index.php/jees

ARTICLE

High-precision Geochronology of Mesozoic Volcanic Rocks from the Ning-Wu Basin, Eastern China: Implications for Geological Evolution

Yan Zhang [1], *Yi Liu* [2*], *Jiannian Zeng* [3], *Yong Zeng* [2]

[1] *Geological Data Archives of Jiangsu Province, Technology Innovation Center for Geological Data Intelligent Application of Jiangsu Province, Nanjing 210018, China*

[2] *Nanjing Center, China Geological Survey, Nanjing 210016, China*

[3] *School of Earth Resources, China University of Geosciences, Wuhan 430074, China*

ABSTRACT

The Ning-Wu Basin is an important part of the Middle-Lower Yangtze River Metallogenic Belt in eastern China. It contains well-preserved Mesozoic volcanic sequences that document significant geodynamic evolution. However, uncertainties surrounding the ages of eruptions and the temporal relationships between the four main volcanic cycles — the Longwangshan, Dawangshan, Gushan and Niangniangshan formations — have hindered our understanding of magmatic pulsation and its connection to iron mineralisation. Here, high-precision LA-ICP-MS zircon U-Pb dating of four fresh volcanic samples (one per formation) reveals weighted mean ages of 132.3 ± 1.0 Ma (Longwangshan; MSWD = 1.3), 130.4 ± 1.6 Ma (Dawangshan; MSWD = 1.3), 128.1 ± 1.9 Ma (Gushan; MSWD = 2.0) and 127.2 ± 1.1 Ma (Niangniangshan; MSWD = 0.23). These dates constrain volcanic activity to the Early Cretaceous Valanginian–Hauterivian interval and show a systematic trend of increasingly younger ages spanning ~8 Ma (133–125 Ma). This magmatism can be subdivided into three phases: initiation (133–132 Ma), peak activity (132–130 Ma) and cessation (128–125 Ma). The episodic volcanism correlates with the accelerating rollback of the Pacific subduction zone, which drives crustal melting and asthenospheric upwelling. Notably, these cycles supplied the thermal energy, fluids and iron-rich melts that were essential for the formation of porphyritic iron deposits in the basin. By establishing a high-resolution chronostratigraphic framework, this study sheds light on the spatiotemporal evolution of the Ning-Wu Basin, elucidating the coupling between crust-mantle dynamics, volcanic cyclicity and ore-forming processes across eastern China's metallogenic belt.

Keywords: Volcanic Rocks; Zircon U-Pb Age; Chronology; Plate Rollback; Ning-Wu Basin

*CORRESPONDING AUTHOR:

Yi Liu, Nanjing Center, China Geological Survey, Nanjing 210016, China; Email: njliuyi025@163.com

ARTICLE INFO

Received: 20 May 2025 | Revised: 17 June 2025 | Accepted: 4 July 2025 | Published Online: 25 July 2025
DOI: https://doi.org/10.30564/jees.v7i7.10115

CITATION

Zhang, Y., Liu, Y., Zeng, J., et al., 2025. High-precision Geochronology of Mesozoic Volcanic Rocks from the Ning-Wu Basin, Eastern China: Implications for Geological Evolution. Journal of Environmental & Earth Sciences. 7(7): 341–352. DOI: https://doi.org/10.30564/jees.v7i7.10115

1. Introduction

The Ning-Wu Basin is a significant component of the Middle-Lower Yangtze River Metallogenic Belt and is regarded as one of the most favorable areas for mineralization. Large-scale development of porphyry iron deposits related to volcanic-subvolcanic rocks has been observed in this region [1–3]. The Ning-Wu Basin is distinguished by a high density of geological surveys, mineral exploration, and scientific research, positioning it as a prominent research site in China. Scholars have engaged in profound discourses on a range of topics, including the source region characteristics of volcanic rocks, magma source regions, and deep dynamic processes. These discourses have been conducted from diverse perspectives, encompassing stratigraphy, petrology, and geochemistry [4–9]. This century has seen significant advancements in precise SIMS or LA-ICP MS zircon U-Pb dating techniques, providing a more precise chronological framework for the volcanic and intrusive rocks in this region [10–17]. However, despite the numerous achievements of previous studies, there is still a lack of systematic and complete precise chronological constraints on the exact timing and duration of the four volcanic cycles within the basin, namely the Longwangshan Formation, Dawangshan Formation, Gushan Formation, and Niangniangshan Formation. This has resulted in divergent interpretations of the development process of the Middle-Lower Yangtze River Metallogenic Belt and the role of deep materials in mineralization [18–23]. To address this, systematic high-precision chronological studies were conducted on the volcanic rocks of the four volcanic cycles in the Ning-Wu Basin. The LA-ICP MS zircon U-Pb dating method was used to test and analyze representative rock samples from each volcanic cycle, obtaining accurate age data. A comprehensive analysis of the temporal sequence of Mesozoic volcanic activities in the Ning-Wu Basin was carried out to explore the relationship between each volcanic cycle and the mineralization of porphyry iron deposits in the Ning-Wu Basin. The large-scale thinning effect of the continental lithosphere in eastern China in this region and its temporal controlling factors were discussed, providing new insights for regional geological evolution theory.

2. Geological Setting

The Ning-Wu Basin is located at the northeastern margin of the Yangtze Block in eastern China (**Figure 1**). The basement is composed of pre-Sinian metamorphic rocks, while the overlying strata are formed by Mesozoic and Cenozoic sedimentary layers, with an exposed area of approximately 1000 km^2.

Since the Mesozoic era, the basin has undergone multiple periods of intense tectono-magmatic activities, resulting in the formation of a thick continental volcanic-sedimentary rock series. These activities are influenced by the subduction of the Pacific Plate towards the Eurasian continent. Among these deposits are abundant porphyritic iron deposits. These deposits are an important type of ore deposit in the Middle-Lower Yangtze River Metallogenic Belt [24,25].

The Mesozoic volcanic rock stratigraphic sequence in the Ning-Wu Basin is complete, consisting of the Longwangshan Formation, Dawangshan Formation, Gushan Formation, and Niangniangshan Formation from bottom to top [1]. The Longwangshan Formation is distributed in the eastern and central uplift areas of the basin, covering approximately 18% of the area. It is a set of purplish-red calc-alkaline trachytic ignimbrite, with a small amount of sedimentary tuff and thin layers of mudstone interbedded. The Dawangshan Formation is the main body of volcanic rocks in the basin, covering about 70% of the area. It is primarily composed of intermediate to intermediate-acid andesitic-dacitic ignimbrite, with a minor presence of trachytic ignimbrite and volcanic breccia interbedded. The Gushan Formation is distributed in the western and south-central parts of the basin, covering approximately 10% of the area. It is a set of intermediate to intermediate-basic basaltic trachyandesitic-andesitic ignimbrite, with a small amount of volcanic breccia and sedimentary tuff interbedded. The Niangniangshan Formation is only found in the Niangniangshan area in the western part of the basin, mainly composed of alkaline volcanic rocks such as leucite phonolite and nosean phonolite.

The vertical variation of the volcanic rock stratigraphic sequence is indicative of changes in the composition and nature of volcanic eruption materials during four distinct stages. Each volcanic cycle initiates with an explosive phase, is succeeded by an effusive phase, and culminates in the volcanic sedimentary phase and subvolcanic activity, denoting the cycle's conclusion.

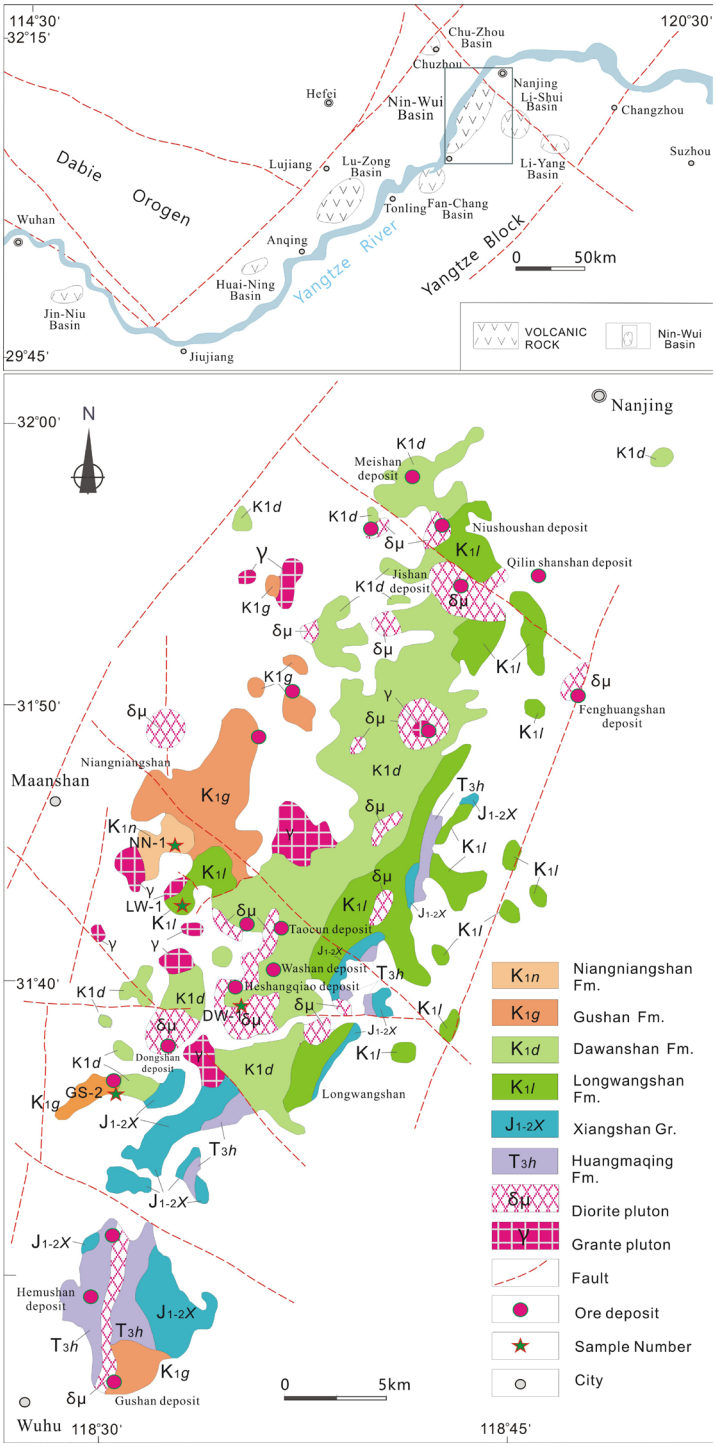

Figure 1. Geology and mineral resources in the Ning-Wu Basin. Modified by Ning-Wu Research Group[1].

3. Sampling and Analytical Methods

The accelerated industrialization and road construction in this region have engendered favorable conditions for the procurement of fresh samples that are shallowly weathered and unaltered. Pursuant to meticulous field geological surveys, a total of four representative samples of considerable thickness and a wide range from each group of volcanic rocks were systematically collected, thereby exemplifying the peaks of large-scale and high-intensity volcanic eruptions. During the sampling process, the representativeness, freshness, and integrity of the samples were thoroughly considered.

LW-1 was collected from the Longwangshan For-

mation near Guaipo Road in Putang Township (N 31°42′47.5″, E 118°33′31.5″). The rock type is gray-brown hornblende trachyte with a porphyritic texture. The phenocrysts primarily comprise alkali feldspar, hornblende, and a trace of pyroxene, while the matrix exhibits a cryptocrystalline structure.

DW-1 was obtained from the Dawangshan Formation located adjacent to the road at Nanshan Quarry, with geographical coordinates of N 31°39′21.0″ and E 118°36′00.7″. It is classified as dark grey trachyandesite, with phenocrysts primarily composed of plagioclase and hornblende. The matrix is primarily constituted by the interweaving of plagioclase microlites.

GS-2 was obtained from the Gushan Formation at Danjingshan on Ma'anshan, with coordinates of N 31°36′17.3″ and E 118°31′07.0″. The specimen is a gray-black massive andesite, with phenocrysts composed of plagioclase and dark minerals. The matrix exhibits a vitreous intersertal texture. The feldspar has undergone sericitization.

NN-1 was collected from the Niangniangshan Formation in the northeastern mountain ravine of Tonging Niangniangshan, with coordinates of N 31°44′57.0″ and E 118°33′28.4″. The specimen is a grey-greyish white nosean phonolite with a pseudo-rhyolitic structure, composed of nosean phonolite breccia, coarse andesite breccia, and tuff components.

The crushing and selection of zircon samples were carried out by the laboratory of the Hebei Regional Institute of Geological and Mineral Exploration. Subsequent to crushing, conventional gravity and magnetic separation methods were employed to screen the zircons. Under a binocular microscope, the zircon particles to be tested were placed in epoxy resin for fixation and then dried to create sample targets. These samples were observed and photographed under transmitted and reflected light with an optical microscope to determine the locations for in situ microanalysis of the zircons. And zircon CL images (**Figure 2**) for dating were formed.

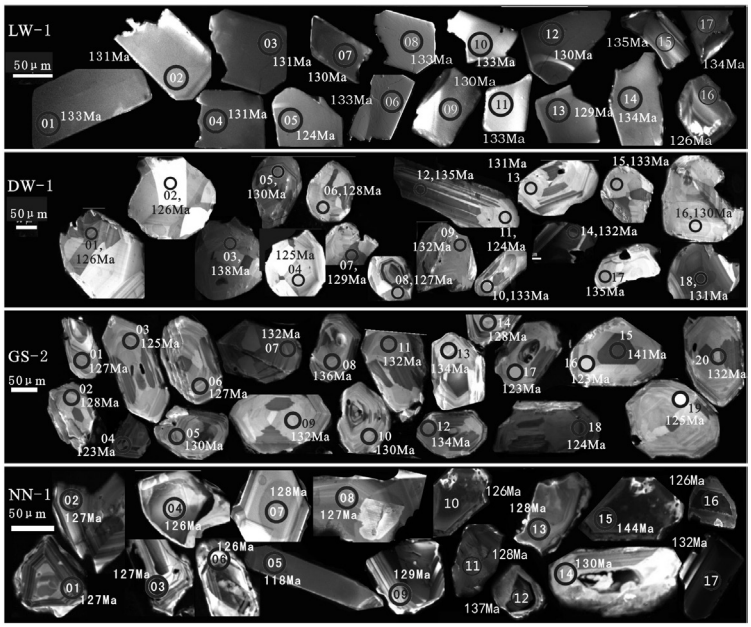

Figure 2. CL image and measurement results of zircon samples from volcanic rocks dated in the Ning-Wu Basin.

The in situ microanalysis of zircon was carried out at the State Key Laboratory of Geological Processes and Mineral Resources (GPMR), China University of Geosciences (Wuhan), using a LA-ICP MS system composed of an Agilent 7500a inductively coupled plasma mass spectrometer and a Geolas 2005 excimer laser ablation system. The laser beam spot diameter used in the system was 24 μm or 32 μm, and helium (He) was used as the carrier gas for the ablated material during the experiment. Which effectively preserves the micro-scale information of the samples. For the data processing of the analysis results obtained from the experiment, Glitter (version 4.0) software was used. The U-Th-Pb isotopic composition analysis employed standard zircon 91500 as an external standard and

NIST610 as an internal standard. For rare earth elements, zircon 91500 was used as an external standard and 91Zr as an internal standard. The specific detailed procedures and principles can be referred to in the relevant technical documents by Liu et al [26]. The age calculation and harmony plotting were implemented through the Isoplot software version 3.7 [27], and the error of the isotopic ratio and the average age of $^{206}Pb/^{238}U$ was set as 1σ. Finally, the weighted $^{206}Pb/^{238}U$ age was obtained using the $^{206}Pb/^{238}U$ ratio.

4. Results

4.1. Sample Selection

A total of four samples were selected for analysis, and the majority of the zircons were found to be light yellow, with a few exhibiting a colorless appearance. The particle shapes were predominantly long prismatic and plate prismatic, with irregular shapes also being observed. The length of the zircon crystals ranged from 60–200μm, the width varied from 30–150μm, and the length-width ratio spanned from 1.5:1–7:1 (**Figure 2**)

With the exception of the LW-1 sample from the Longwangshan Formation, the zircons in the other three samples all exhibit relatively obvious oscillatory zoning characteristics under cathodoluminescence. The analysis results indicate that the Th/U ratios (**Figure 2**) are as follows: for the LW-1 sample, the Th/U ratio ranges from 2.62–5.31; for the DW-1 sample, the ratio ranges from 0.57–1.50; for the GS-2 sample, the ratio ranges from 0.66-1.04; and for the NN- The Th/U ratio of the NN-1 sample ranges from 0.61–9.67, with a point NN-1–11 Th/U ratio of 0.2, which is less than the common ratio of magmatic zircons but greater than the Th/U ratio of metamorphic zircons. Notably, the ratio of point NN-1–17 is as high as 52.86, which is interpreted as late-stage magmatic zircons and was excluded from age calculations. It is noteworthy that these ratios are all significantly higher than the Th/U ratio of metamorphic zircons (< 0.1), and fall within the range of Th/U ratios of magmatic zircons (> 0.4). This observation indicates that these selected zircons are all have a typical magmatic origin.

4.2. Analysis Results

In the analysis of sample LW-1, 15 of the 17 data points exhibited $^{206}Pb/^{238}U$ values concentrated within the 129 ± 2.0–135 ± 2.0 Ma range (**Table 1**). The weighted average age of $^{206}Pb/^{238}U$ for these data points is 132.3 ± 1.0 Ma (MSWD = 1.3). In the concordia diagram (**Figure 3a**), the data points are clustered on and around the concordant curve, and the weighted average age of $^{206}Pb/^{238}U$ has a high degree of consistency. This age is considered to be the crystallization age of the Longwangshan volcanic cycle within the Ning-Wu Basin. For data point LW-1–5, the presence of inclusions has been observed, with notable peaks detected in both the heavy rare earth elements and the Eu element. These peaks may be indicative of the presence of apatite inclusions.

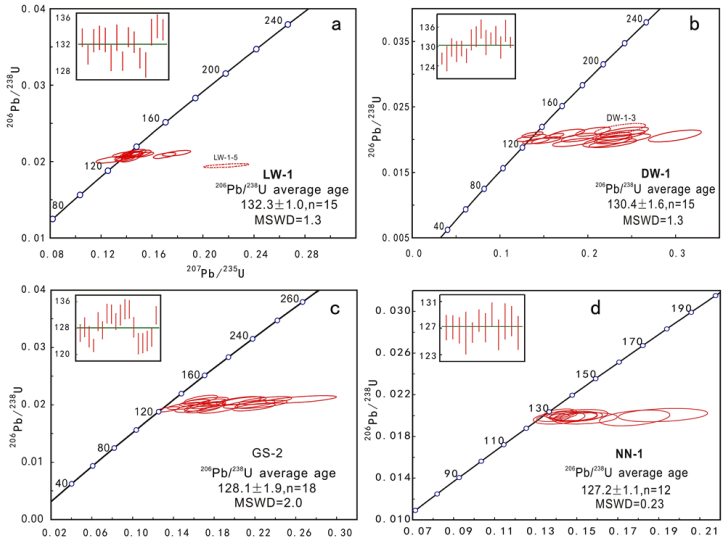

Figure 3. The LA-ICP MS zircon U-Pb geochronological harmony diagram of volcanic rocks in the Ning-Wu Basin.

Table 1. LA-ICP MS Zircon U-Pb Dating Analysis Data of Volcanic Rocks from the Ning-Wu Basin (Age in Ma).

Point No.	^{232}Th	^{238}U	Th/U	^{207}Pb/^{206}Pb		^{207}Pb/^{235}U		^{206}Pb/^{238}U		^{208}Pb/^{232}Th		^{206}Pb/^{238}U		^{207}Pb/^{235}U		^{208}P/^{232}Th	
	Conc. /10^{-6}			Ratio	1σ	Ratio	1σ	Ratio	1σ	Ratio	1σ	Age	1σ	Age	1σ	Age	1σ
LW-1 (Sample Number)																	
01	4549.0	993.2	4.58	0.0535	0.0019	0.1535	0.0052	0.0209	0.0002	0.0067	0.0001	133	1	145	5	135	2
02	6520.8	1492.5	4.37	0.0486	0.0016	0.1378	0.0047	0.0205	0.0002	0.0062	0.0001	131	1	131	4	125	2
03	8120.1	1579.5	5.14	0.0506	0.0019	0.1453	0.0053	0.0208	0.0003	0.0065	0.0001	133	2	138	5	130	2
04	7085.8	1414.9	5.01	0.0501	0.0016	0.1452	0.0052	0.0209	0.0003	0.0067	0.0001	133	2	138	5	134	3
05	6304.0	1384.2	4.55	0.0813	0.0044	0.2182	0.0117	0.0195	0.0002	0.0063	0.0001	124	1	200	10	126	3
06	6490.1	1609.5	4.03	0.0501	0.0020	0.1439	0.0056	0.0208	0.0003	0.0067	0.0002	133	2	137	5	134	3
07	5303.1	1382.6	3.84	0.0509	0.0019	0.1428	0.0051	0.0204	0.0003	0.0065	0.0002	130	2	136	5	132	3
08	5694.3	1934.3	2.94	0.0494	0.0018	0.1424	0.0053	0.0209	0.0003	0.0066	0.0001	133	2	135	5	133	3
09	3814.6	718.5	5.31	0.0491	0.0018	0.1385	0.0050	0.0203	0.0002	0.0067	0.0001	130	1	132	4	135	2
10	4306.6	1018.4	4.23	0.0475	0.0019	0.1371	0.0055	0.0209	0.0002	0.0067	0.0001	133	1	130	5	136	2
11	5263.1	1258.0	4.18	0.0596	0.0022	0.1698	0.0059	0.0208	0.0002	0.0068	0.0001	133	2	159	5	136	3
12	8407.7	1641.8	5.12	0.1065	0.0037	0.3009	0.0101	0.0204	0.0002	0.0064	0.0001	130	2	267	8	129	2
13	3024.4	832.3	3.63	0.0462	0.0031	0.1283	0.0082	0.0202	0.0003	0.0062	0.0001	129	2	123	7	124	3
14	3246.5	1207.2	2.69	0.0518	0.0019	0.1505	0.0058	0.0210	0.0003	0.0066	0.0002	134	2	142	5	133	3
15	4124.7	1575.6	2.62	0.0498	0.0020	0.1460	0.0062	0.0212	0.0003	0.0064	0.0001	135	2	138	6	129	3
16	9564.9	1827.7	5.23	0.1672	0.0081	0.4526	0.0206	0.0198	0.0002	0.0059	0.0001	126	1	379	14	119	2
17	4206.0	1347.5	3.12	0.0620	0.0027	0.1793	0.0074	0.0211	0.0002	0.0067	0.0001	134	2	167	6	134	2
DW-1 (Sample Number)																	
01	162.4	208.1	0.78	0.0514	0.0036	0.1407	0.0100	0.0198	0.0003	0.0068	0.0003	126	2	134	9	137	5
02	56.5	75.5	0.75	0.0924	0.0096	0.2225	0.0186	0.0198	0.0006	0.0071	0.0012	126	4	204	15	144	24
03	71.5	87.4	0.82	0.0844	0.0073	0.2370	0.0191	0.0216	0.0006	0.0078	0.0004	138	4	216	16	157	9
04	69.5	101.8	0.68	0.0698	0.0063	0.1845	0.0163	0.0196	0.0004	0.0072	0.0004	125	3	172	14	146	8
05	63.3	97.7	0.65	0.0702	0.0058	0.1904	0.0137	0.0203	0.0004	0.0072	0.0004	130	3	177	12	144	8
06	57.1	81.4	0.70	0.0927	0.0085	0.2398	0.0211	0.0201	0.0005	0.0065	0.0004	128	3	218	17	131	8
07	144.7	153.7	0.94	0.0500	0.0044	0.1359	0.0112	0.0203	0.0004	0.0064	0.0004	129	2	129	10	129	8
08	155.9	186.4	0.84	0.0561	0.0042	0.1527	0.0111	0.0199	0.0003	0.0062	0.0002	127	2	144	10	126	5
09	67.3	87.3	0.77	0.0875	0.0077	0.2373	0.0186	0.0207	0.0005	0.0072	0.0004	132	3	216	15	146	8
10	104.8	127.8	0.82	0.1587	0.0388	0.4740	0.1277	0.0208	0.0005	0.0101	0.0007	133	3	394	88	202	13
11	55.5	73	0.76	0.0936	0.0081	0.2286	0.0179	0.0195	0.0004	0.0155	0.0086	124	3	209	15	311	171
12	149.5	133.3	1.12	0.0744	0.0051	0.2061	0.0132	0.0212	0.0005	0.0071	0.0003	135	3	190	11	144	5
13	57.8	73.3	0.79	0.1153	0.0086	0.2993	0.0199	0.0206	0.0006	0.0066	0.0004	131	4	266	16	132	8
14	221.6	284.4	0.78	0.0481	0.0029	0.1371	0.0081	0.0208	0.0003	0.0066	0.0002	132	2	130	7	134	4
15	76.9	100.9	0.76	0.0628	0.0047	0.1765	0.0132	0.0209	0.0005	0.0069	0.0003	133	3	165	11	139	7
16	47.1	70.8	0.67	0.0867	0.0054	0.2298	0.0132	0.0203	0.0005	0.0068	0.0004	130	3	210	11	138	9
17	48.1	84.6	0.57	0.0874	0.0070	0.2415	0.0183	0.0211	0.0005	0.0078	0.0005	135	3	220	15	156	9
18	722.5	480.6	1.50	0.0576	0.0027	0.1623	0.0071	0.0206	0.0003	0.0068	0.0002	131	2	153	6	137	3
GS-2 (Sample Number)																	
01	75.1	114	0.66	0.0578	0.0048	0.1530	0.0123	0.0198	0.0004	0.0057	0.0003	127	3	145	11	114	6
02	62.4	85.1	0.73	0.0874	0.0083	0.2259	0.0169	0.0201	0.0005	0.0076	0.0004	128	3	207	14	152	8
03	52.9	68	0.78	0.0654	0.0049	0.1706	0.0132	0.0196	0.0005	0.0063	0.0003	125	3	160	11	127	7
04	223	215	1.04	0.0512	0.0030	0.1348	0.0075	0.0192	0.0003	0.0060	0.0002	123	2	128	7	121	4
05	96.1	118	0.82	0.0655	0.0039	0.1772	0.0095	0.0204	0.0004	0.0066	0.0003	130	3	166	8	132	6

Table 1. *Cont.*

Point No.	^{232}Th	^{238}U	Th/U	^{207}Pb/^{206}Pb		^{207}Pb/^{235}U		^{206}Pb/^{238}U		^{208}Pb/^{232}Th		^{206}Pb/^{238}U		^{207}Pb/^{235}U		^{208}P/^{232}Th	
	Conc. /10^{-6}			Ratio	1σ	Ratio	1σ	Ratio	1σ	Ratio	1σ	Age	1σ	Age	1σ	Age	1σ
06	77.8	103	0.75	0.0660	0.0045	0.1740	0.0114	0.0200	0.0004	0.0059	0.0003	127	3	163	10	119	5
07	62.3	90.3	0.69	0.0813	0.0059	0.2303	0.0171	0.0208	0.0005	0.0074	0.0004	132	3	210	14	149	8
08	74.1	100.5	0.74	0.0734	0.0049	0.2096	0.0129	0.0213	0.0004	0.0082	0.0004	136	3	193	11	166	8
09	58.8	76.7	0.77	0.0767	0.0062	0.2090	0.0144	0.0207	0.0004	0.0061	0.0003	132	3	193	12	122	7
10	77.7	108	0.72	0.0591	0.0040	0.1608	0.0099	0.0204	0.0004	0.0062	0.0003	130	2	151	9	126	6
11	55.9	77.1	0.73	0.0749	0.0055	0.2042	0.0146	0.0207	0.0005	0.0064	0.0004	132	3	189	12	129	8
12	96.1	113	0.85	0.0592	0.0040	0.1670	0.0108	0.0210	0.0005	0.0073	0.0003	134	3	157	9	147	6
13	82.6	109	0.76	0.0912	0.0080	0.2651	0.0230	0.0210	0.0004	0.0077	0.0004	134	3	239	18	154	9
14	55.6	70.3	0.79	0.0803	0.0070	0.2142	0.0167	0.0201	0.0005	0.0061	0.0003	128	3	197	14	124	6
15	72.0	74	0.97	0.1250	0.0108	0.4008	0.0404	0.0222	0.0007	0.0113	0.0009	141	4	342	29	228	18
16	50.5	71.1	0.71	0.0722	0.0055	0.1834	0.0132	0.0193	0.0005	0.0062	0.0003	123	3	171	11	125	7
17	67.4	90.1	0.75	0.0632	0.0047	0.1688	0.0117	0.0193	0.0005	0.0059	0.0003	123	3	158	10	120	6
18	52.3	75.2	0.69	0.0644	0.0059	0.1597	0.0121	0.0194	0.0005	0.0069	0.0004	124	3	150	11	139	8
19	54.2	79.5	0.68	0.0833	0.0061	0.2191	0.0138	0.0196	0.0004	0.0076	0.0004	125	3	201	11	154	8
20	62.2	79.7	0.78	0.0633	0.0061	0.1717	0.0147	0.0207	0.0004	0.0066	0.0003	132	3	161	13	134	7
NN-1 (Sample Number)																	
01	422.2	694.2	0.61	0.0560	0.0027	0.1522	0.0069	0.0199	0.0003	0.0066	0.0002	127	2	144	6	133	5
02	722.9	478.7	1.51	0.0544	0.0029	0.1482	0.0079	0.0199	0.0003	0.0063	0.0001	127	2	140	7	126	3
03	335.9	547.2	0.61	0.0156	0.0074	0.0427	0.0201	0.0198	0.0003	0.0048	0.0005	127	2	42.5	19.6	96	10
04	206.7	145.7	1.42	0.0675	0.0045	0.1783	0.0113	0.0198	0.0005	0.0064	0.0003	126	3	167	10	129	5
05	531.7	702.5	0.76	0.0533	0.0025	0.1351	0.0060	0.0185	0.0002	0.0057	0.0001	118	1	129	5	115	3
06	742.9	1212.4	0.61	0.0504	0.0019	0.1387	0.0054	0.0198	0.0002	0.0063	0.0002	126	1	132	5	127	3
07	971.3	100.4	9.67	0.0513	0.0018	0.1428	0.0049	0.0201	0.0003	0.0063	0.0002	128	2	136	4	127	3
08	718.2	100.1	7.17	0.0553	0.0026	0.1495	0.0069	0.0199	0.0003	0.0063	0.0002	127	2	142	6	128	3
09	1464.8	2100.6	0.70	0.0511	0.0020	0.1419	0.0053	0.0202	0.0003	0.0067	0.0002	129	2	135	5	136	3
10	340.6	462.5	0.74	0.0570	0.0039	0.1540	0.0104	0.0197	0.0004	0.0064	0.0002	126	2	145	9	129	5
11	181.4	896.9	0.20	0.0698	0.0050	0.1920	0.0144	0.0201	0.0004	0.0072	0.0003	128	3	178	12	144	7
12	757.4	305.8	2.48	0.0519	0.0016	0.1544	0.0050	0.0214	0.0003	0.0065	0.0002	137	2	146	4	132	4
13	370.7	251.7	1.47	0.0547	0.0034	0.1512	0.0093	0.0201	0.0004	0.0067	0.0002	128	2	143	8	135	5
14	124.1	2094.3	0.06	0.0626	0.0060	0.1693	0.0151	0.0204	0.0005	0.0076	0.0003	130	3	159	13	153	7
15	300.5	98.1	3.06	0.0460	0.0031	0.1429	0.0094	0.0226	0.0004	0.0074	0.0002	144	2	136	8	149	5
16	688.1	98.2	7.01	0.0523	0.0033	0.1414	0.0084	0.0198	0.0004	0.0065	0.0002	126	2	134	7	131	4
17	23668.2	447.8	52.86	0.0482	0.0013	0.1384	0.0037	0.0207	0.0002	0.0065	0.0001	132	2	132	3	130	3

For sample DW-1, among its 18 data points, 15 data points ^{206}Pb/^{238}U are concentrated in 126 ± 2.0–135 ± 3.0 Ma (**Table 1**). The data points are observed to be concentrated on and around the concordant curve in the concordia diagram (**Figure 3b**), and its weighted average age of ^{206}Pb/^{238}U is 130.4 ± 1.6 Ma (MSWD = 1.3). This age is considered to reflect the crystallization age of the Dawangshan volcanic cycle in the Ning-Wu Basin. It is noteworthy that the ^{206}Pb/^{238}U age value of data point DW-1–03 is 138.0 ± 4 Ma, which may imply that this point has inherited the age characteristics of zircons from the Longwangshan cycle.

For sample GS-2, the ^{206}Pb/^{238}U values of 18 data points fall within the range of 123 ± 3.0–134 ± 3.0 Ma (**Table 1**). These data points exhibit a clustered distribution along and surrounding the concordant curve in the concordia diagram (**Figure 3c**), and their weighted average age of ^{206}Pb/^{238}U is 128.1 ± 1.9 Ma (MSWD = 2.0). This data can

be regarded as the representative of the crystallization age of the Gusan volcanic cycle in the Ning-Wu Basin. Among the data points, GS-2–08 is situated within the oscillatory zoning region of the zircon and is in proximity to the core, suggesting that its age value may be a composite of multiple ages. Conversely, GS-2–15 is positioned near the core of the zircon, indicating that its age may be the inherited zircon age.

The analysis of sample NN-1 reveals that among its 17 data points, 12 data points $^{206}Pb/^{238}U$ are concentrated in 126 ± 3.0–132 ± 2.0 Ma (**Table 1**). The concordia diagram reveals that these data points are concentrated on and around the concordant curve (**Figure 3d**), and their weighted average age of $^{206}Pb/^{238}U$ is 127.2 ± 1.1 Ma (MSWD = 0.23). This age is interpreted to represent the crystallization age of the Niangniangshan volcanic cycle in the Ning-Wu Basin. Additionally, the $^{206}Pb/^{238}U$ age values of data points NN-1–12 and NN-1–15 are 137.0 ± 2 Ma and 144 ± 2 Ma, respectively, suggesting that these two data points may have inherited the age information of zircons.

5. Discussion

5.1. Constraints of Chronological Results

The high-precision LA-ICP-MS zircon U-Pb ages presented in this study (Longwangshan 132.3 ± 1.0 Ma, MSWD = 1.3; Dawangshan 130.4 ± 1.6 Ma, MSWD = 1.3; Gushan 128.1 ± 1.9 Ma, MSWD = 2.0; and Niangniangshan 127.2 ± 1.1 Ma, MSWD = 0.23) robustly constrain Mesozoic volcanic cycles in the Ning-Wu Basin to 133–125 Ma (8 Ma interval). The age of the Niangniangshan Formation (127.2 ± 1.1 Ma) contrasts with previous reports of 118.3 ± 3.0 Ma [16] and 133.1 ± 3.2 Ma [28]. This discrepancy is attributed to analytical limitations in earlier studies (e.g. altered zircons). Our data, derived from unaltered samples with magmatic Th/U ratios (> 0.4), provide a more accurate result. An inherited zircon from the Longwangshan cycle (Dawangshan sample DW-1–03: 138.0 ± 4.0 Ma) was identified, which is consistent with the proximity to older crustal materials [12,15]. This outlier does not affect the primary weighted mean age (MSWD = 1.3), which aligns with pulsed basin evolution.

These ages (Valanginian–Hauterivian, Early Cretaceous) and volcanic rock associations define four distinct volcanic cycles: Longwangshan (133–132 Ma), Dawangshan (132–130 Ma), Gushan (130–128 Ma) and Niangniangshan (128–125 Ma). This chronology indicates a progression of volcanic activity from initial incubation through to peak eruption and eventual cessation. These results are consistent with existing geochronological data (**Table 2**) and earlier palynological studies [1,29]. Subvolcanic rocks and hypabyssal intrusions (genetically linked to porphyritic iron ores) reveal three coeval magmatic pulses at 131.7–130.7 Ma, 128.2–127.8 Ma and 127.0–125.0 Ma [12,14–16], confirming the spatiotemporal coupling of intrusive and extrusive magmatism.

Crucially, the ages of the formations exhibit a systematic trend of becoming younger from Longwangshan to Niangniangshan, indicating cyclical volcanism. The short interval (~2 Myr) between the volcanism at Longwangshan and Dawangshan reflects intense Early Cretaceous tectono-magmatic activity, whereas the prolonged gap (~3 Myr) between the volcanism at Gushan and Niangniangshan suggests tectonic deceleration or stress-field reconfiguration. Post-Niangniangshan volcanic quiescence marks the end of major activity.

These results resolve ambiguities in the timing of Ning-Wu volcanism and demonstrate superior accuracy to earlier studies. The refined chronology provides a precise temporal framework for Mesozoic magmatic evolution and ore genesis in the Middle-Lower Yangtze River Metallogenic Belt.

Table 2. Main Results of Chronological Studies on Volcanic Rock Series in the Ning-Wu Basin.

No.	Unit (Fm.)	Lithology	Age (Ma)	Method	Reference
1	Niangniangshan Fm.	Amygdaloid	118.3 ± 3.0	LA-ICP MS U-Pb	[16]
2	Niangniangshan Fm.	Amygdaloid	126.6 ± 1.1	LA-ICP MS U-Pb	[15]
3	Niangniangshan Fm.	Amygdaloid	127.2 ± 1.1	LA-ICP MS U-Pb	[This paper]
4	Niangniangshan Fm.	Breccia tuff meltrock	130.6 ± 1.1	LA-ICP MS U-Pb	[12]
5	Niangniangshan Fm.	Amygdaloid	133.1 ± 3.2	Rb-Sr isochron	[28]
6	Gusan Fm.	Andesite	128.0 ± 2	LA-ICP MS U-Pb	[16]
7	Gusan Fm.	Andesite	128.1 ± 1.9	LA-ICP MS U-Pb	[This paper]
8	Gusan Fm.	Coarse andesite	128.2 ± 1.3	SHRIMP U-Pb	[14]
9	Gusan Fm.	Coarse andesite	128.5 ± 1.8	SHRIMP U-Pb	[14]

Table 2. *Cont.*

No.	Unit (Fm.)	Lithology	Age (Ma)	Method	Reference
10	Gusan Fm.	Pyroxene andesite	129.5 ± 0.8	LA-ICP MS U-Pb	[15]
11	Gusan Fm.	Pyroxene coarse andesite	131.5 ± 1.0	LA-ICP MS U-Pb	[16]
12	Gusan Fm.	Andesite	131.7 ± 1.1	LA-ICP MS U-Pb	[22]
13	Dawangshan Fm.	Pyroxene coarse andesite	126.7 ± 0.9	^{40}Ar-^{39}Ar	[5]
14	Dawangshan Fm.	Coarse andesite	127 ± 3Ma	SHRIMP U-Pb	[11]
15	Dawangshan Fm.	Trachy andesite	130.3 ± 0.9	SHRIMP U-Pb	[14]
16	Dawangshan Fm.	Tuff	130.4 ± 1.0	LA-ICP MS U-Pb	[16]
17	Dawangshan Fm.	Trachyandesite	130.4 ± 1.6	LA-ICP MS U-Pb	[This paper]
18	Dawangshan Fm.	Andesite	130.6 ± 1.6	LA-ICP MS U-Pb	[22]
19	Dawangshan Fm.	Andesite	131.7 ± 1.2	LA-ICP MS U-Pb	[16]
20	Dawangshan Fm.	Hornblende andesite	132.2 ± 1.6	LA-ICP MS U-Pb	[15]
21	Dawangshan Fm.	Pyroxene andesite	132.6 ± 1.8	LA-ICP MS U-Pb	[22]
22	Longwangshan Fm.	Coarse andesite	129.1 ± 2.6	LA-ICP MS U-Pb	[17]
23	Longwangshan Fm.	Coarse andesite	131 ± 4Ma	SHRIMP U-Pb	[11]
24	Longwangshan Fm.	Volcanic breccia	131.2 ± 3.6	LA-ICP MS U-Pb	[17]
25	Longwangshan Fm.	Hornblende trachyte	132.3 ± 1.0	LA-ICP MS U-Pb	[This paper]
26	Longwangshan Fm.	Volcanic rock	134.0 ± 2.7	LA-ICP MS U-Pb	[16]
27	Niangniangshan Fm.	Hornblende andesite	134.8 ± 1.3	LA-ICP MS U-Pb	[15]

5.2. Regional Correlation with Adjacent Basins

The Middle-Lower Yangtze Metallogenic Belt comprises NE-striking fault basins accompanied by coeval Early Cretaceous volcanism. The Ningwu Basin (133–125 Ma) acts as a chronostratigraphic anchor and constrains four volcanic cycles (Longwangshan to Niangniangshan Formations), which are dominated by trachyandesitic compositions.

Fanchang Basin: Three eruptive cycles (Zhongfencun, Chisha and Kedoushan formations; 133–130 Ma [12]) of trachytic–andesitic assemblages show full temporal overlap with the Longwangshan–Dawangshan transition in the Ningwu Basin. Lujiang Basin: Four volcanic phases (Longmenyuan, Zhuanqiao, Shuangmiao and Fushan formations; 134.8–127.1 Ma [30]) share a near-identical termination age of ~125 Ma with Ningwu, as evidenced by analogous trachyandesite–trachyte suites and diagnostic pseudoleucite phonolite layers. Jinniu Basin: Three volcanic units (the Majiashan, Lingxiang and Dashi formations; 130–125 Ma [31]) exhibit bimodal basalt–rhyolite assemblages, indicating delayed initiation but synchronous cessation with Ningwu.

Temporally, volcanic onset progresses westward: The Lujiang Basin initiated the earliest (134.8 Ma), followed by the Ningwu Basin (133 Ma) and the Fanchang Basin (133 Ma), with the Jinniu Basin commencing the latest (130 Ma). Crucially, all basins converge at the cessation point of ~125 Ma, as validated by regional data [12,30,31].

These findings confirm the validity of the Ningwu chronology as a foundational reference for the metallogenic belt and resolve previously ambiguous inter-basin correlations. The synchronous termination of volcanism across spatially distinct basins supports the hypothesis that the tectonic regime transition of continental crust in eastern China was the dominant mechanism[32–34], offering a chronostratigraphic framework for reconstructing Mesozoic tectonic evolution in the region.

5.3. Implications for Geological Evolution

The volcanic rocks of the Middle-Lower Yangtze region predominantly comprise shoshonitic series lithologies (trachybasalts, basaltic trachyandesites, trachytes, trachyandesites and phonolites). These rocks exhibit enrichment in LILE (Rb, Ba, K, Th, U and Pb) and LREE, as well as depletion in HFSE (Nb, Ta, Ti, P and Y) and HREE. They also have low levels of transitional elements (Sc, V, Cr and Ni) [7,9,12]. Negative Eu anomalies in select samples further distinguish this signature from that of mid-ocean ridge basalt (MORB) or ocean island basalt (OIB), reflecting instead arc-like or crustally contaminated magmatism [16,35].

Sr-Nd-Hf isotopes exhibit compositions that are weakly enriched with elevated radiogenic Pb, which is consistent with the assimilation of continental crust during arc-related magma ascent [28,36]. These features indicate derivation from the partial melting of an enriched mantle

source, followed by fractional crystallisation and crustal contamination [36,37]. This geochemical fingerprint correlates with Pacific plate subduction dynamics. During the Mesozoic era, the oblique subduction of the Izanagi Ridge beneath Eurasia drove lithospheric evolution in stages: flat-slab subduction (pre-early Cretaceous) → post-subduction thickening → slab rollback with lithospheric thinning (late early to late Cretaceous). Multiple rollback events occurred as the slab steepened [19,20,23,25].

The regional Cu-Au-Fe mineralisation peak (150–120 Ma) coincided with asthenospheric upwelling resulting from slab reorganization. Ningwu volcanism (133–125 Ma) marked the peak of slab steepening, where the steep edges of the slab facilitated: basaltic underplating, enhanced asthenospheric flow and crustal anatectism, driving large-scale volcanic eruptions. Zircon Hf-O isotopic data ($\varepsilon Hf(t) = -5.5$ to -10.2; $\delta^{18}O = 5.0–6.5$ ‰ [9,35]) confirm the presence of hybrid melts originating from an enriched lithospheric mantle and an ancient lower crust. This mixing peaked at 132–125 Ma, generating iron-rich magmas[33,36]. After 125 Ma, the eastward rollback of the Paleo-Pacific slab initiated regional extension and lithospheric thinning, bringing an end to volcanism at the same time as the cessation of the Niangniangshan cycle. This tectonic shift defined the structural framework of the Ningwu Basin, linking its evolution to Pacific subduction dynamics and Mesozoic lithospheric stretching in eastern China.

6. Conclusions

1. This study establishes a high-precision geochronological framework for Mesozoic volcanic cycles in the Ning-Wu Basin. Four distinct eruptive phases are constrained over an 8 Myr interval (133–125 Ma). The progressive rejuvenation of the formations indicates pulsed volcanism, with brief (~2 Myr) and extended (~3 Myr) intervals between cycles, suggesting variable tectonic and magmatic activity.
2. The Ning-Wu Basin acts as a chronostratigraphic anchor for the Middle-Lower Yangtze Metallogenic Belt, revealing the simultaneous end of volcanism in neighbouring basins (Lujiang, Fanchang and Jinniu) at around 125 million years ago (Ma). Despite westward decreasing initiation ages (134.8 Ma to 130 Ma), this synchronicity underscores a unified tectonic driver, likely the transition from flat-slab subduction to rollback of the Paleo-Pacific slab.
3. Shoshonitic volcanism (enriched LILE/LREE and depleted HFSE/HREE) and Sr-, Nd-, Hf- and Pb-isotopes trace hybrid melts from an enriched lithospheric mantle and an ancient lower crust. This activity peaked during slab steepening (133–125 Ma). The abrupt cessation of volcanism after 125 Ma correlates with lithospheric thinning induced by slab rollback, marking the end of major Fe-rich magmatism and basin evolution.
4. Future studies should address the following: (1) The exact mechanisms linking slab rollback to basin-specific volcanic cyclicity. (2) The role of crustal heterogeneity in modulating magma compositions. (3) Potential triggers for the westward migration of volcanic onset.

Author Contributions

Conceptualization, Y.Z.; methodology, J.Z.; investigation, Y.Z. and Y.L.; resources: J.Z. and Y.L.; writing-original draft preparation, Y.Z.; writing-review and editing, Y.Z. and Y.Z. (Yong Zeng); project administration: Y.Z.; funding acquisition, Y.Z. and Y.L. All authors have read and agreed to the published version of the manuscript.

Funding

This work was supported by The Special Funds for Natural Resource Development in Jiangsu Province (2200113-35) and The Central Financial Geological Survey Project of the China Geological Survey (DD20230800702).

Institutional Review Board Statement

Not applicable.

Informed Consent Statement

Not applicable.

Data Availability Statement

Data are contained within the article.

Acknowledgments

We sincerely appreciate the support from the Geologi-

cal Data Archives of Jiangsu Province (GDA) and Nanjing Center, China Geological Survey (CGS) for providing us with a research base and technical support for our work. We are grateful to Director Chen Jie of GDA, Ph.D Zhang Ming of CGS for discussing the relevant problems and difficulties we encountered during the field investigation and writing process, from which we have derived profound inspiration. The authors have reviewed and edited the output and take full responsibility for the content of this publication.

Conflicts of Interest

The authors declare no conflict of interest.

References

[1] Ning-Wu Research Group, 1978. Magnetite porphyry deposits in Ning-Wu area [in Chinese]. Geological Publishing House: Beijing, China. pp. 1–196.

[2] Chang, Y.F., Liu, X.P., Wu, Y.C., 1991. The Copper-Iron Belt of the Lower and Middle Reaches of the Changjiang River [in Chinese]. Geological Publishing House: Beijing, China. pp. 1–379.

[3] Liu, Y., Zeng, Y., Shi, H.F., et al., 2018. Analysis of the prospecting potential of Zhuyuanshan-type iron deposit in the northern Nangjing-Wuhu area. Journal of Geology. 42(1), 32–39.

[4] Xing, F.M., 1996. Petrological and Nd, Sr, Pb isotopic evidence for genesis of Mesozoic magmatic rocks in Nanjing-Wuhu area [in Chinese]. Acta Petrologica et Mineralogica. 15(2), 126–137.

[5] Ma, F., Jiang, S.Y., Jiang, Y.H., et al., 2006. Pb isotope research of porphyrite Fe deposits in the Ning-Wu area. Acta Geologica Sinica. 80(2), 279–288.

[6] Hu, J.P., Jiang, S.Y., 2010. Zircon U-Pb dating and Hf isotopic compositions of porphyrites from the Ning-Wu Basin and their geological implications. Journal of Geology in Higher Education Institutions. 16(3), 294–305. DOI: https://doi.org/10.3969/j.issn.1006-7493.2010.03.003

[7] Liu, Z., Huang, D.Z., Liu, Y.H., et al., 2014. Geochemical characteristics and genesis of volcanic and sub-volcanic rocks from porphyrite-type iron deposits in Ning-Wu metallogenic province, eastern China: Constraints from elements. Journal of Central South University. 21(7), 2866–2876. DOI: https://doi.org/10.1007/s11771-014-2252-5

[8] Yu, J., Che, L., Wang, T., 2015. Alteration, oxygen isotope and fluid inclusion study of the Meishan iron oxide-apatite deposit, SE China. Mineralium Deposita. 50(7), 847–869. DOI: https://doi.org/10.1007/s00126-015-0577-0

[9] Duan, C., Li, Y.H., Mao, J.W., et al., 2024. Magma source transformation of multi-stage volcanism in Ning-Wu ore district, eastern China: Evidence from zircon Hf-O isotopes of intrusions. Mineral Deposits. 43(2), 227–243.

[10] Ye, S.Q., 2000. A discussion on the time of volcanic rock system for Gushan F.M. North section of Ning-Wu. Jiangsu Geology. 24(4), 210–214.

[11] Zhang, Q., Jian, P., Liu, D.Y., et al., 2003. SHRIMP dating of volcanic rocks from Ning-Wu area and its geological implications. Science in China Series D-Earth Sciences. 46(8), 830–837. DOI: https://doi.org/10.1007/BF02879526

[12] Yan, J., Liu, H.Q., Song, C.Z., et al., 2009. Zircon U-Pb geochronology of the volcanic rocks from Fanchang-Ning-Wu volcanic basins in the Lower Yangtze region and its geological implications. Chinese Science Bulletin. 54(16), 2895–2904. DOI: https://doi.org/10.1007/s11434-009-0110-x

[13] Fan, Y., Zhou, T.F., Yuan, F., et al., 2010. Geochronology of the diorite porphyrites in Ning-Wu basin and their metallogenic significances [in Chinese]. Acta Petrologica Sinica. 26(9), 2715–2728.

[14] Hou, K.J., Yuan, S.D., 2010. Zircon U-Pb age and Hf isotopic composition of the volcanic and sub-volcanic rocks in the Ning-Wu basin and their geological implications [in Chinese]. Acta Petrologica Sinica. 26(3), 888–902.

[15] Zhou, T.F., Fan, Y., Yuan, F., et al., 2013. Geology and geochronology of magnetite-apatite deposits in the Ning-Wu volcanic basin, eastern China. Journal of Asian Earth Sciences. 66, 90–107. DOI: https://doi.org/10.1016/j.jseaes.2012.12.030

[16] Wang, L.J., Wang, R.C., Yu, J.H., et al., 2014. Geochronology, geochemistry of volcanic-intrusive rocks in the Ning-Wu basin and its geological implications [in Chinese]. Acta Geologica Sinica. 88(7), 1247–1272.

[17] Li, X.S., Yuan, F., Deng, Y.F., et al., 2020. Geochronology, geochemistry and metallogenic potential of trachyandesite from Longwangshan copper mine spot in the middle section of Ning-Wu Basin [in Chinese]. Journal of Hefei University of Technology (Natural Science). 43(7), 975–987. DOI: https://doi.org/10.3969/j.issn.1003-5060.2020.07.019

[18] Zhou, X.M., Li, W.X., 2000. Origin of Late Mesozoic igneous rocks in Southeastern China: Implications for lithosphere subduction and underplating of mafic

magmas. Tectonophysics. 326(3–4), 269–287. DOI: https://doi.org/10.1016/S0040-1951(00)00120-7

[19] Li, Z.X., Li, X.H., 2007. Formation of the 1300 km-wide intracontinental orogen and postorogenic mag-matic province in Mesozoic South China: A flat-slab subduction model. Geology. 35(2), 179–182. DOI: https://doi.org/10.1130/G23193A.1

[20] Ling, M.X., Wang, F.Y., Ding, X., et al., 2009. Cretaceous ridge subduction along the Lower Yangtze River Belt, eastern China. Economic Geology. 104(2), 303–321.

[21] Zhang, Y., Guo, K.Y., Zeng, J.N., 2013. Zircon U-Pb dating of the orebearing porphyrites and its geological significance for the Washan iron deposit, Nanjing-Wuhu Basin. Resources Survey & Environment. 34(4), 228–233.

[22] Yang, Y.H., Wang, L.J., Zhang, S.Q., 2015. Zircon U-Pb dating and Lu-Hf isotopic analysis of volcanic rocks from the Nanjing-Wuhu Basin in volcanism peak period [in Chinese]. Journal of Geology. 39(4), 556–566.

[23] Sun, W.D., Ling, M.X., Yang, X.Y., et al., 2010. Ridge subduction and porphyry copper-gold mineralization: An overview. Science China Earth Sciences. 53, 475–484. DOI: https://doi.org/10.1007/s11430-010-0024-0

[24] Mao, J.W., Wang, Y.T., Lehmann, B., et al., 2005. Molybdenite Re-Os and albite 40Ar/39Ar dating of Cu-Au-Mo and magnetite porphyry systems in the Yangtze River valley and metallogenic implications. Ore Geology Reviews. 29(3–4), 307–324. DOI: https://doi.org/10.1016/j.oregeorev.2005.11.001

[25] Li, S.Z., Suo, Y.H., Li, X.Y., et al., 2019. Mesozoic tectono-magmatic response in the East Asian ocean-continent connection zone to subduction of the Paleo-Pacific Plate. Earth-Science Reviews. 192, 91–137. DOI: https://doi.org/10.1016/j.earscirev.2019.03.003

[26] Liu, Y.S., Hu, Z.C., Zong, K.Q., et al., 2010. Reappraisal and refinement of zircon U-Pb isotope and trace element analyses by LA-ICP-MS. Chinese Science Bulletin. 55(15), 1535–1546. DOI: https://doi.org/10.1007/s11434-010-3052-4

[27] Ludwig, K.R., 2008. ISOPLOT 3.7: A Geochronological Toolkit for Microsoft Excel. Berkeley Geochronology Center: Oakland, CA, USA. pp. 1–74.

[28] Yan, J., Liu, J., Li, Q., et al., 2015. In situ zircon Hf-O isotopic analyses of Late Mesozoic magmatic rocks in the Lower Yangtze River Belt, Central eastern China: Implications for petrogenesis and geodynamic evolution. Lithos. 227, 57–76. DOI: https://doi.org/10.1016/j.lithos.2015.03.013

[29] Zhao, Y.C., 1990. Stratigraphic division of Mesozoic volcanic strata and their characteristics in Nanjing-Wuhu area. Chinese Journal of Geology. 3, 243–258. DOI: https://doi.org/10.1007/BF02919267

[30] Zhou, T.F., Fan, Y., Yuan, F., et al., 2008. Geochronology of the volcanic rocks in the Luzong basin and its significance. Science in China Series D-Earth Sciences. 51(10), 1470–1482. DOI: https://doi.org/10.1007/s11430-008-0111-7

[31] Xie, G.Q., 2006. SHRIMP zircon U-Pb dating for volcanic rocks of the Dasi Formation in southeast Hubei Province, middle-lower reaches of the Yangtze River and its implications [in Chinese]. Chinese Science Bulletin. 51(19), 9. DOI: https://doi.org/10.3321/j.issn:0023-074X.2006.19.011

[32] Xing, G.F., Li, J.Q., Duan, Z., et al., 2021. Mesozoic-Cenozoic volcanic cycle and volcanic reservoirs in East China. Journal of Earth Science. 32(4), 742–765. DOI: https://doi.org/10.1007/s12583-021-1476-1

[33] Tang, Y.J., Zhang, H.F., Ying, J.F., et al., 2013. Rapid eruption of the Ning-Wu volcanics in eastern China: Response to Cretaceous subduction of the Pacific plate. Geochemistry, Geophysics, Geosystems. 14, 1703–1721. DOI: https://doi.org/10.1002/ggge.20082

[34] Dong, Q., Li, Z.Y., Fan, H.H., et al., 2017. LA-ICP-MS U-Pb zircon dating of gabbro from Jiangmiao of Ning-Wu Basin in the middle and lower Yangtze region and its geological significance [in Chinese]. Mineralogy and Petrology. 37(4), 88–94.

[35] Duan, C., Li, Y., Mao, J., et al., 2023. Zircon U-Pb ages, Hf-O isotopes and trace elements of the multi-volcanism in the Ning-Wu ore district, eastern China: Implications for the magma evolution and fertility of iron oxide-apatite (IOA) deposits. Gondwana Research. 116, 149–167. DOI: https://doi.org/10.1016/j.gr.2022.12.009

[36] Huo, H.D., Yang, Z.L., Hong, W.T., 2024. Inverse reaction rim of biotite in early Cretaceous nosean phonolite of Niangniangshan, Ningwu Basin: Mineralogical evidence of magma mixing triggered volcanic eruption. East China Geology. 45(1), 115–133. DOI: https://doi.org/10.16788/j.hddz.32-1865/P.2024.01.009

[37] Li, J.H., Zhang, Y.Q., Dong, S.W., et al., 2014. Cretaceous tectonic evolution of South China: A preliminary synthesis. Earth-Science Reviews. 134, 98–136. DOI: https://doi.org/10.1016/j.earscirev.2014.03.008